Design, Synthesis, and Isomerization Studies of Light-Driven Molecular Motors for Single Molecular Imaging

Chen, Jiawen; Vachon, Jerome; Feringa, B.L.

Published in:
Journal of Organic Chemistry

DOI:
10.1021/acs.joc.8b00654

Publication date:
2018

JOC The Journal of Organic Chemistry

Article

Cite This: J. Org. Chem. 2018, 83, 6025−6034

pubs.acs.org/joc

Design, Synthesis, and Isomerization Studies of Light-Driven Molecular Motors for Single Molecular Imaging

Jiawen Chen,* Jérôme Vachon, and Ben L. Feringa*

Stratingh Institute for Chemistry, University of Groningen, Nijenborgh 4, 9747AG Groningen, The Netherlands

Supporting Information

ABSTRACT: The design of a multicomponent system that aims at the direct visualization of a synthetic rotary motor at the single molecule level on surfaces is presented. The synthesis of two functional motors enabling photochemical rotation and fluorescent detection is described. The light-driven molecular motor is found to operate in the presence of a fluorescent tag if a rigid long rod (32 Å) is installed between both photoactive moieties. The photochemical isomerization and subsequent thermal helix inversion steps are confirmed by ^{1}H NMR and UV−vis absorption spectroscopies. In addition, the tetra-acid functioned motor can be successfully grafted onto amine-coated quartz and it is shown that the light responsive rotary motion on surfaces is preserved.

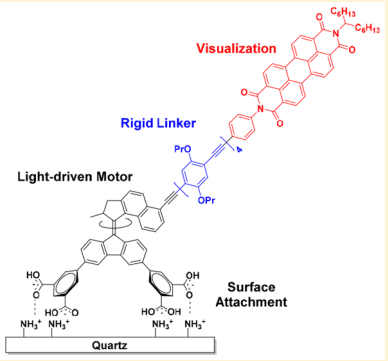

1. INTRODUCTION

Nature features a large collection of molecular motors that are able to operate complex biological processes which are crucial to sustain proper functioning of our organisms, i.e. fuel production, transport, mobility, and a plethora of other dynamic functions.[1] These processes are accomplished with high efficiency and selectivity under precise control at the molecular level. For example, ATP synthase contains a genuine molecular rotary motor to enable the process of synthesizing or hydrolyzing ATP.[2] Other examples include the flagella rotary motor,[3] which induces the movement of bacterial cells, whereas linear motors[4] are involved in muscle contraction and intracellular transport among others.[5]

Inspired by the variety of protein-based motors in Nature, a series of artificial molecular motors have been developed over the past decades.[6−18] These synthetic motors are designed to perform controlled rotary and linear motion at the molecular level by utilizing chemical, photochemical, electrical, and thermal energy input. Our group's effort toward achieving controlled motion focuses on light-driven molecular motors based on chiral overcrowded alkenes.[19,20] By applying light and heat, these motors can undergo continuous motion due to well-defined conformational and configurational changes, resulting in a repetitive unidirectional rotary cycle. Light-driven molecular motors have been used to dynamically control other functions, while remaining its key rotary motion, to achieve a variety of applications. Selected examples include dynamic control over the chiral space of catalysts,[21] conversion of rotary into translational motion with a nanocar,[22] dynamic control over cell membrane permiability,[23] macroscopic contraction of a hydrogel,[24] helical reorganization and amplification in liquid crystals,[25,26] dynamic supramolecular double helical assemblies,[27] and artificial muscle function.[28]

In spite of the rapid development of molecular motors, one major obstacle to harness the motion generated by these motors to perform work is Brownian motion,[29,30] i.e. random motion due to the molecular collisions and vibrations that perpetually disrupt any directed motion. Recent advances toward surface assembly of molecules provide important approaches to overcome this problem.[31−34] By confining molecular motors on surfaces, the relative rotation of one part of the molecule with respect to the other can be converted to absolute rotation of the rotor relative to the surface and collective motion can be harnessed.[35,36] It would be highly desirable to construct a system that allows visualization of the controlled motion of a single molecular motor. By direct visualization of the single molecular rotary motion, two important issues might be addressed: (1) both positional and orientational order of the motors can be determined, and (2) the motion of a single molecular motor, rather than the random Brownian motion, can be controlled and studied in real time, which can provide ample mechanistic details about the motion. These two fundamental issues are therefore arguably crucial for further understanding, design, and applications of molecular motors.

Yoshida, Kinosita and co-workers reported a landmark achievement by direct visualization of the rotary motion of a single natural rotary molecular motor by fluorescence microscopy.[37] The ATPase motor was mounted to a surface through histidine tags introduced in the F_1 subunit (Figure 1a). A long actin filament with a fluorescent tag was attached to the F_0 subunit. Addition of ATP induced the rotation of the F_0

Received: March 14, 2018
Published: May 9, 2018

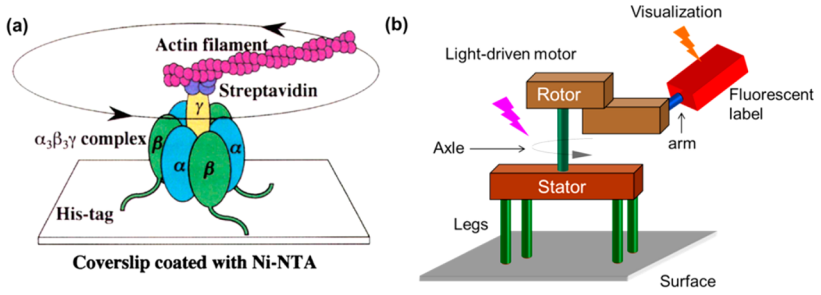

Figure 1. (a) Schematic illustration of the structure of F_0F_1-ATPase grafted on a surface for visualization of unidirectional rotation (reproduced with permission from ref 37, Copyright 1997 Nature Publishing Group). (b) Conceptual design of a synthetic surface-bound light-driven molecular motor for single molecule imaging.

Scheme 1. Light Driven Molecular Motors: (a) Representative Structure of a Second Generation Molecular Motor; (b) First Design of a PBI-Labelled Surface-Bound Molecular Motor 1a

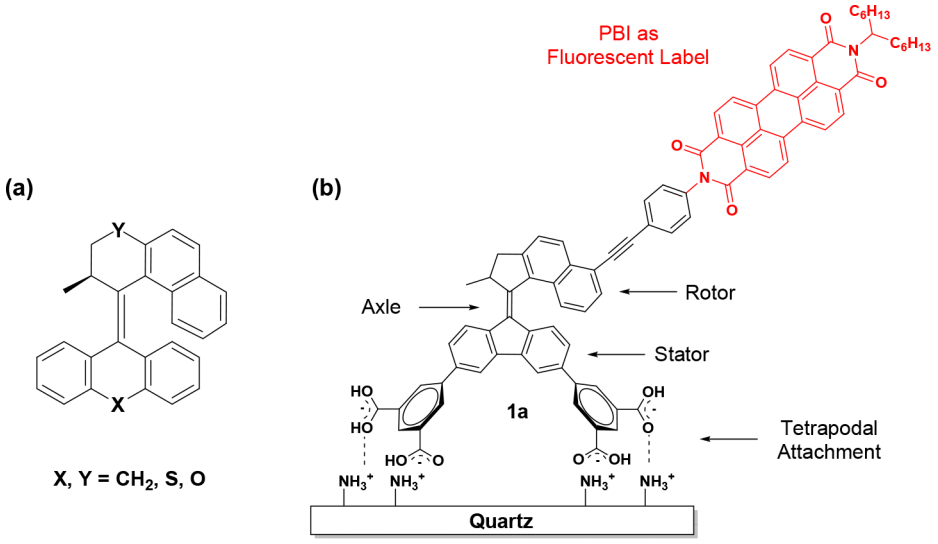

subunit and thereby of the actin filament, and the directional motion was monitored by fluorescence microscopy in real time.

An important challenge was whether direct visualization of the rotating motion of an entirely synthetic motor at the single molecular level is feasible? As a crucial step to meet this challenge, we aimed to design and synthesize a molecular motor suitable for single molecular imaging while attached to surfaces. Inspired by the pioneering work of Yoshida and Kinosita, and encouraged by a recent report of Hofkens[38] in which the thermal rotation of a surface-bound synthetic tripodal rotor which is equipped with legs to allow detection by defocused wide-field imaging was studied, we envisioned a design shown in Figure 1b. The lower half of a light-driven molecular motor attached to a surface serves as the stator, while the upper half can be considered the rotor. The rotor part is equipped with a rigid arm and fluorescent label. Two different irradiation wavelengths can be applied to the system: one triggers the rotation of the motor while the other excites the fluorescent moiety. In principle, the stepwise rotary cycle of the motor, powered by light and heat, induces rotation of the fluorescent group, which can be followed by a change in fluorescent anisotropy using defocused wide field fluorescence microscopy.

The total synthesis of such a highly complicated molecule is not a trivial task and requires considerable synthetic effort since several different functional groups need to be installed in a facile and efficient way. More importantly, all the functional groups involved should operate orthogonally without interfering with one another in such a multicomponent system, in particular interactions of chromophores. Finally the system needs to be assembled on a surface and rotary motion should not be compromised by surface interference, i.e. excited state quenching, etc. In the present report, we focus on the design, total synthesis, and solution isomerization studies of two target motors. The proper functioning of each component in these two motors is investigated, and the structural modifications to preserve the rotary motion of the motor are discussed.

2. RESULTS AND DISCUSSION

2.1. Design. The structure of second generation light-driven molecular motors based on overcrowded alkenes (Scheme 1a) has been modified to alter the rotary motion and speed for different purposes.[20] In the present study, the motor core structure with a five-membered cyclopentene and a fluorenene lower half was chosen (Scheme 1b) since motors of similar structures are found to have rotary speeds of 1−3 min at rt,[20] which is suitable for microscopic measurements and allows for easy functionalization at both upper and lower halves.

The choice of the fluorescent label is also of major importance in the construction of the designed system (Figure 1, Scheme 1) and is based on the following criteria: (1) high fluorescence quantum yield and molar absorptivity; (2) absorption and emission maxima at wavelengths that do not

DOI: 10.1021/acs.joc.8b00654
J. Org. Chem. 2018, 83, 6025−6034

Scheme 2. Retrosynthesis of Motor 1a

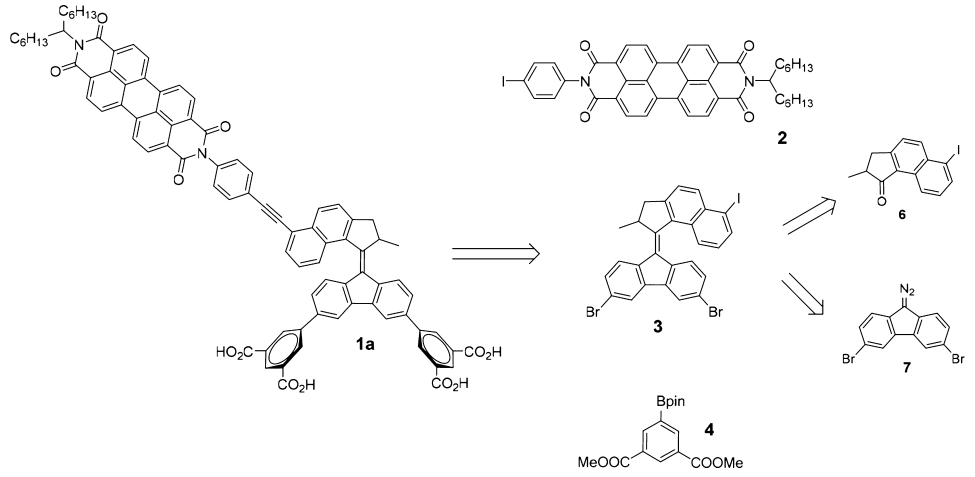

Scheme 3. Synthetic Route of Motor 1a

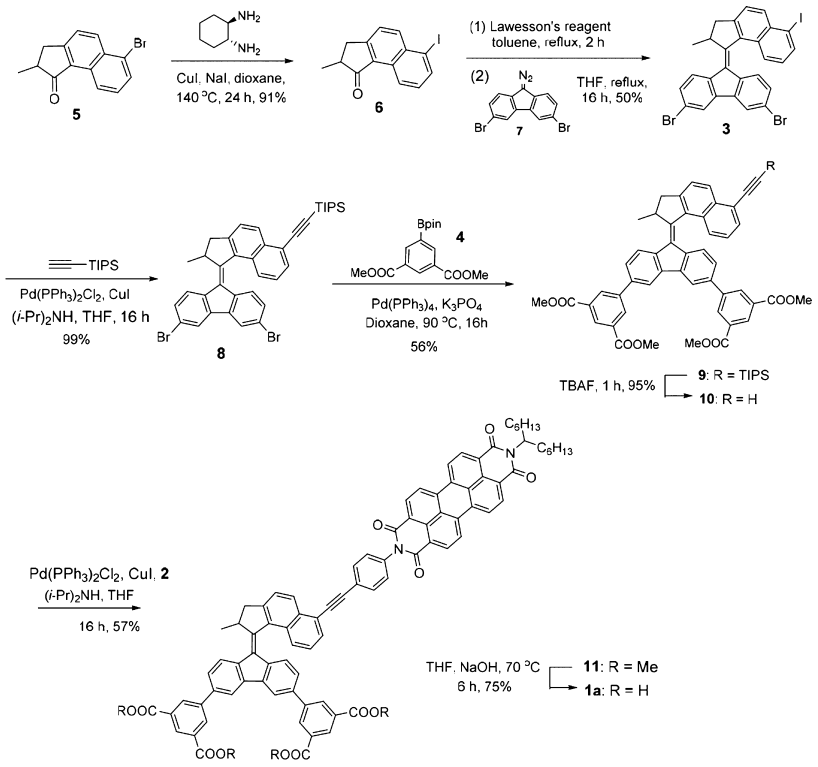

interfere with the wavelengths required to induce the rotation of the molecular motor: preferably above 480 nm; (3) high chemical and photochemical stability; (4) facile functionalization. Perylene bisimide (PBI) derivatives have been shown to possess exceptional chemical, thermal, and photochemical stabilities.[39−41] In addition, the fluorescence quantum yield of PBI is found to be close to unity.[42,43] Due to these properties, PBI has been used widely, for instance in dye sensitizers based solar cells[44,45] and they are important components in light-emitting diodes[46−49] and field effect transistors.[50−52] Furthermore, PBI has been successfully applied in single-molecule spectroscopy for investigation of the optical behavior of multichromophoric dendrimers[53,54] and rotation of a surface-bound rotor.[38] In addition, two PBI units have been attached on both sides of a light-driven molecular motor to achieve dynamic control over the intramolecular H-stacking of PBI.[55] The studies showed that distinct properties of PBI (high fluorescence quantum yield, photo- and thermal stability) are preserved, and the introduction of a PBI unit does not interfere with the motor's function. Therefore, PBI is considered as a good candidate as the fluorescent label of choice in the present design (Scheme 1b).

Several methods of attaching molecular motors onto surfaces have been developed in our group, using both covalent[35,36] and noncovalent approaches.[56] Assembly of a tetra-acid-functionalized motor to amine-coated surfaces involving multiple electrostatic interactions provides an appealing strategy.[56] This approach does not require the introduction of any chemicals for activation prior to attachment, which significantly helps to improve the cleanness of the sample preparation for single molecular microscopic measurements. Furthermore, the rotary motion of a motor on surfaces is well preserved via this

DOI: 10.1021/acs.joc.8b00654
J. Org. Chem. 2018, 83, 6025−6034

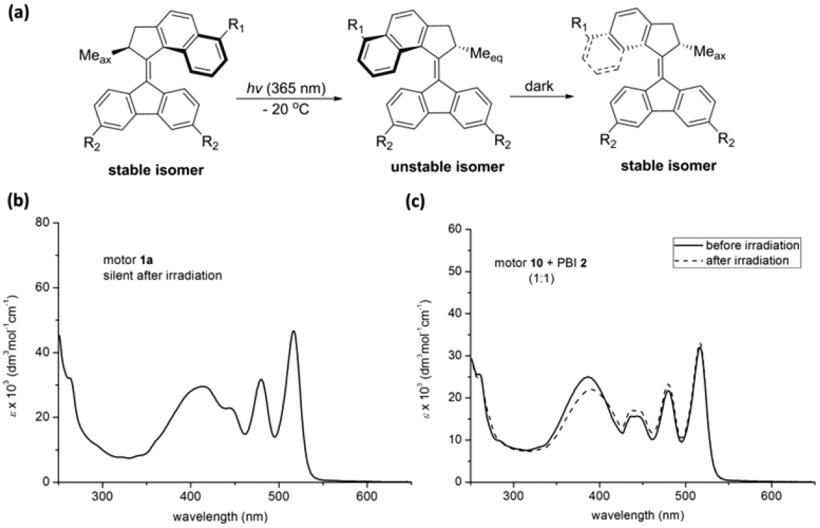

Figure 2. (a) Photochemical and thermal helix inversion steps of light-driven molecular motors. Only one enantiomer is shown; the two stable isomers are identical but viewed from different angles. (b, c) UV−vis absorption spectra (CH_2Cl_2, −20 °C) before and after irradiation (λ_{max} = 365 nm) of (b) motor **1a** and (c) a 1:1 mixture of motor **10** and PBI **2**.

surface immobilization approach.[56] Based on the above considerations, motor **1a** was proposed in our initial design (Scheme 1b). This multifunctional motor comprises several key parts: (1) an overcrowded alkene based rotary motor as a central core; (2) a PBI unit in the rotor half of the motor as the fluorescent label; (3) two isophthalic acid groups in the stator half for surface attachment.

2.2. Synthesis of 1a. Essential to the retrosynthetic analysis of **1a**, shown in Scheme 2, is that various functional groups need to be installed to the motor core in an orthogonal way. A multifunctionalized motor **3** was proposed as a key intermediate. We anticipate that advantage can be taken of the iodo-bromo selectivity in some cross-coupling reactions, e.g. Sonogashira reaction and Suzuki reactions, to allow the upper or lower half of the motor core being functionalized independently and selectively.

The synthesis (Scheme 3) started from a bromo ketone **5**,[20] which was converted to the corresponding more reactive aryl iodide **6** by an aromatic Finkelstein reaction, employing the conditions developed by Buchwald.[57] It should be noted that it is required that the reaction temperature is kept at 140 °C for at least 24 h to ensure full conversion. The resulting iodo ketone **6** was treated with Lawesson's reagent in toluene heated at reflux for 2 h to generate the corresponding thioketone which was immediately treated with a THF solution of dibromo diazo compound **7**.[56] The mixture was heated at reflux overnight, giving rise to the key intermediate overcrowded alkene **3**. Next, a Sonogashira coupling of **3** was performed with 1 equiv of triisopropylsilyl acetylene at rt for 16 h in the presence of $Pd(PPh_3)_2Cl_2$, CuI, and $(i\text{-}Pr)_2NH$. Monosubstituted product **8** was isolated as the exclusive product, leaving the two bromo substituents at the lower half intact. These bromo substituents were then replaced by two isophthalic acid methyl ester moieties via a Suzuki cross-coupling reaction with bis-substituted phenyl B-pin-ester **4**,[58] providing **9** in 56% yield. Deprotection of the triisopropylsilyl group was achieved by treating **9** with TBAF, affording **10** which bears a terminal acetylene. Motor **10** was then coupled with a reported aryl iodide **2**[59] bearing a PBI unit by Sonagashira reaction, giving rise to a tetra-ester **11**, which was subsequently hydrolyzed in the presence of a base to generate the target molecule **1a**.

2.3. UV−vis Studies of 1a. Upon irradiation with UV-light (λ_{max} = 365 nm), the molecular motor is expected to undergo a photoinduced isomerization around the central double bond. Like related second generation motor motors,[20] during this process, the molecule is converted from a stable isomer to an unstable isomer in which the methyl group at the stereogenic center is forced to adopt an energetically unfavored pseudoequatorial orientation (Figure 2a). A thermal helix inversion step is followed to release the structural strain, resulting in the original stable state with the methyl group at the stereocenter in a more favorable pseudoaxial orientation. Surprisingly, irradiation of motor **1a** in DCM for 2 h showed no spectral changes neither by UV/vis absorption (Figure 2b) nor by ^{1}H NMR spectroscopy. The above observations suggest that the light-induced rotary motion of the motor is inhibited in this case. To further study this phenomenon, control experiments were performed to establish the effect of the PBI unit on the photochemical transformation. Motor **10**, which is the intermediate before coupling to the PBI unit, was mixed with PBI **2** in a 1:1 ratio in a CH_2Cl_2 solution and subsequently irradiated for 2 h. The UV/vis spectra showed a red shift of the bands around 370 nm (Figure 2c), which is an indication of the formation of the unstable isomer of **10**.[60] After warming the mixture to rt in the dark, the original spectra could be regenerated, indicating that the unstable isomer of **10** was converted to its stable isomer by thermal helix inversion. Based on the above control experiment, we propose that direct attachment of the PBI unit to the motor core by a monoacetylene linker quenches the photochemistry of the motor.

Previously, it has been reported that in some cases fluorescence quenching can take place between PBI and other chromophores due to intramolecularly photoinduced electron transfer (PET).[61−63] Müllen and De Schryver have observed that, by increasing the distance between PBI and other chromophores, PET could be suppressed.[61] Hence, in the present study, a linker of sufficient length is required between the motor core and PBI unit to preserve the motor's rotary

DOI: 10.1021/acs.joc.8b00654
J. Org. Chem. 2018, 83, 6025−6034

motion as well as the uncompromised PBI emission. The flexible long alkyl chain linker which has been used in our previous study[55] on first generation rotary motors with a pending fluorescent group does not meet the requirement of our current design. Instead, a rigid long rod-like linker is needed (Figure 3). Phenyl-ethynylene oligomers (PEO) are

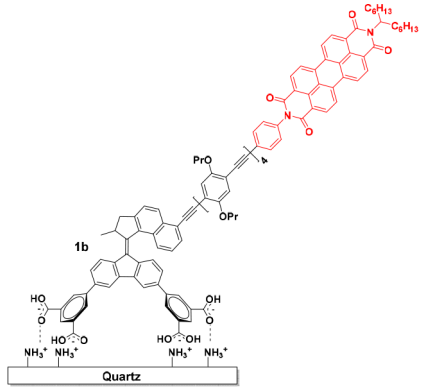

Figure 3. Second design of a surface bound molecular motor **1b**, bearing a rigid long arm between the motor core and PBI label.

considered good candidates due to their shape persistence.[64] Furthermore, according to previous studies in our group, the introduction of PEO does not exert a significant influence on the rotary motion of the molecular motor.[65] Therefore, motor **1b** (Scheme 4) was proposed as our second design, in which a rigid PEO tetramer of 32 Å in length is installed at the rotor to connect the motor core and PBI unit. Each of the PEO units contains two propyl side chains to improve the solubility of the oligomers.

2.4. Synthesis of 1b. The synthesis of the tetramer **12** has been reported by Ziener and Godt[64] and our group[65] via a step-by-step synthesis using Sonogashira cross-coupling methodology. Next, the *p*-iodophenyl-PBI unit **2** was coupled to **12** in the presence of $Pd(PPh_3)_2Cl_2$, CuI, and $(i\text{-Pr})_2NH$ at rt overnight to provide PBI **13** with a rigid linker in 65% yield (Scheme 4). Motor precursor **10** with a terminal acetylene (see Scheme 3) was then coupled with **13** at 80 °C in the presence of $Pd(Ph_3)_4$, CuI, and $(i\text{-Pr})_2NH$ in toluene for 16 h. The tetra-ester **14** could be isolated in 58% yield, which was subsequently hydrolyzed in the presence of a base to generate the tetra-acid motor **1b**.

2.5. ^{1}H NMR Studies. To determine if the second target motor **1b** is able to function properly, ^{1}H NMR studies were performed. Figure 4 displays a partial ^{1}H NMR spectrum of motor **1b** in CD_2Cl_2 solution. The signals of the aliphatic protons H_a, H_b, and H_c and the protons of the Me-group at the stereogenic center are distinctive features for the motor moiety. The doublet at 2.9 ppm is considered to be proton H_a since only a negligible coupling is expected between H_a and H_c due to their relative orientations as a result of the conformation of the five-membered ring.[60] In addition, the double doublet at 4.4 ppm can be assigned to H_b, due to the fact that H_b couples not only to its geminal proton H_a but also to vicinal proton H_c. The multiplet at 4.4 ppm is assigned as proton H_c, as a result of coupling with the protons of the methyl group and proton H_b. Furthermore, the doublet at 1.4 ppm can be assigned to the methyl group at the stereogenic center. The broad signals around 4.0 to 4.2 ppm are due to the alkyl side chains of the rigid tetramer. A solution of **1b** in CD_2Cl_2 was irradiated (λ = 365 nm) at −20 °C and distinct changes were observed in the spectrum, indicating the formation of a new isomer which was identified as unstable-**1b** (Figure 4b). Notably, H_a shifts from 2.9 ppm (doublet) to 3.3 ppm (double doublet). Unstable-**1b** adopts a different conformation than that of stable-**1b**, which allows the coupling between H_a and H_c. The new absorption at 3.7 ppm can be assigned to H_b in the unstable isomer. Furthermore, the signal of the methyl group was observed to shift from 1.4 to 1.6 ppm, which confirms the conformational change of the methyl group from a pseudoaxial orientation in the stable isomer to a pseudoequatorial orientation in the unstable isomer. The photostationary state (PSS) was reached after extended irradiation for 2 h. The ratio was determined to be 7:3 (unstable-**1b**/stable-**1b**), by integration of the signals for proton H_a in the stable isomer and the unstable isomer. Keeping the sample overnight at room temperature under exclusion of light led to recovery of the original spectrum (Figure 4a), indicating the occurrence of the thermal helix inversion to convert unstable-**1b** to stable-**1b**.[60]

2.6. UV−vis Spectroscopy Studies. The rotary motion of motor **1b** was also studied in solution by UV/vis absorption spectroscopy. Figure 5 displays a UV/vis absorption spectrum of stable **1b** in CH_2Cl_2 solution (Figure 5a, solid line). The broad absorption band around 425 nm can be attributed to the

Scheme 4. Synthesis of Motor 1b

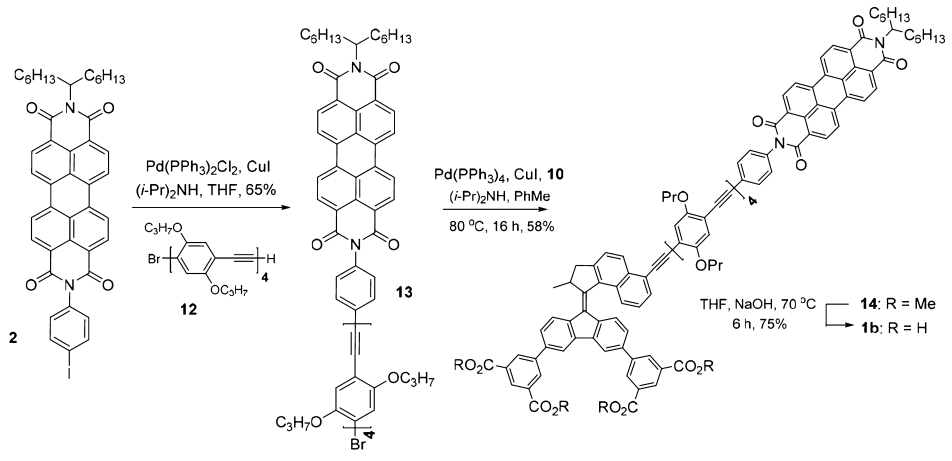

DOI: 10.1021/acs.joc.8b00654
J. Org. Chem. 2018, 83, 6025−6034

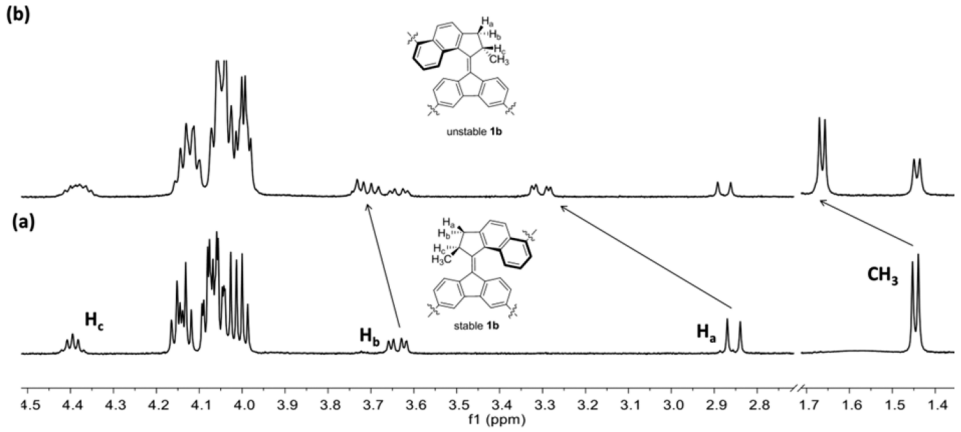

Figure 4. Aliphatic region of the ^{1}H NMR spectra of motor **1b** (CD_2Cl_2, −20 °C, $c = 10^{-3}$ M) (a) stable-**1b**, before irradiation (365 nm); (b) PSS mixture after irradiation.

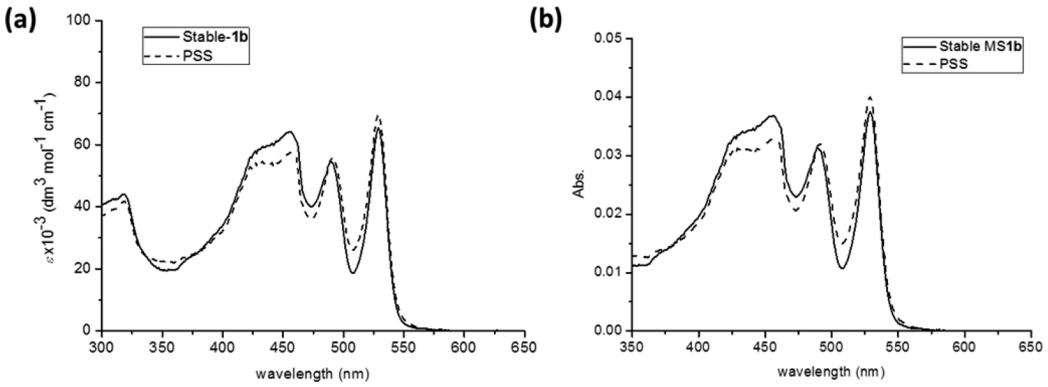

Figure 5. UV/vis absorption spectra of (a) motor **1b** (CH_2Cl_2, 0 °C), stable isomer (solid line) and unstable isomer at PSS (dashed line); (b) **MS-1b** (quartz, 4 °C) before (solid line) and after irradiation (dashed line).

absorption of the rigid tetramer in **1b**. Three characteristic absorption bands of the PBI unit were observed: 456, 490, and 524 nm, which correspond to the 0−2, 0−1, and 0−0 electronic transitions of the PBI unit, respectively.[55] The sample was then irradiated at λ = 365 nm, resulting in a decrease of absorption around 440 nm together with an increased absorption from 480 to 510 nm (Figure 5a, dashed line). This spectral change is consistent with that of a structurally similar motor, indicating the formation of the unstable isomer.[60] The PSS was reached after extended irradiation for 1 h, and an isosbestic point was maintained at 489 nm (Figure 5a). The PSS mixture was kept in the dark at rt overnight, and the change in UV/vis absorption spectrum indicated full conversion to the original state. This reversed process indicates the occurrence of the thermal helix inversion step, in accordance with the ^{1}H NMR studies. The rate of the process was followed by UV/vis absorption spectroscopy at different temperatures, and by Eyring analysis (Supporting Information, Figure S1), a half-life of 148 s at rt was obtained, as well as the Gibbs free energy of activation ($\Delta^{\ddagger}G°$ = 84.5 kJ/mol) at rt, the enthalpy of activation ($\Delta^{\ddagger}H°$ = 72.8 kJ/mol), and entropy of activation ($\Delta^{\ddagger}S°$ = −41.5 J/K·mol). The obtained half-life is similar to those of structurally related second generation motors,[60] suggesting that in this case the rotary motion of motor **1b** is fully preserved. Most importantly, it indicates that a rigid linker with sufficient length is crucial for maintenance of the rotary behavior of a motor when a PBI unit is introduced, showing that the fluorophore does not compromise the rotary function.

2.7. Rotary Motion of Motor 1b on Surfaces. In order to study the rotary motion of motor **1b** on surfaces, surface-attached motor assemblies **MS-1b** (MS = Motor on Surfaces) were prepared. Self-assembly of a tetra-acid functionalized motor on amine-coated quartz surfaces by electrostatic interaction has been developed in our group previously.[56] Therefore, following the reported procedure, the quartz slides with amine-functionalized surfaces were immersed in a DMF solution (10^{-4} M) of **1b** at rt overnight. After extensive rinsing with DMF, water, and MeOH, the functionalized quartz slides were dried under a stream of argon. The freshly prepared slides were then submitted for UV/vis studies. Figure 5b shows a UV/vis absorption spectrum of **MS-1b** (solid line), in which the major absorption band and the absorption profile are similar to that observed in solution (Figure 5a). Characteristic absorptions for the motor (420 nm) and PBI (456 nm, 490 nm, 524 nm) could be observed, indicating the successful attachment of motor **1b** to the amine-coated surfaces. After irradiation of **MS-1b** for 15 min, similar spectral changes were observed as that of the solution, indicating the formation of the unstable **MS-1b**. Keeping the motor-functionalized slides in the dark overnight resulted in a full reversal of the spectra, which indicates the thermal helix inversion step takes place. The above results indicate that the rotary motion of motor **1b** is preserved when it is grafted to a amine-functionalized quartz surface.

DOI: 10.1021/acs.joc.8b00654
J. Org. Chem. 2018, 83, 6025−6034

3. CONCLUSIONS

The conceptual design of a multicomponent system that allows for direct visualization of rotary motion of a synthetic light-driven molecular motor on surfaces is presented. Two molecules **1a** and **1b**, comprising intrinsic motor and fluorescent moieties that should operate independently, were designed and prepared via a multistep synthesis route to assess the proper functioning of these multicomponent motors in solution. While the first designed motor **1a** shows no rotary motion when the motor and PBI unit are connected directly, our modified design, i.e. motor **1b**, which bears a rigid tetramer linker between the PBI unit and motor core to prevent PET, displayed the expected light-driven rotation. Both ^{1}H NMR and UV−vis absorption spectroscopic studies of **1b** confirmed the photochemical and subsequent thermal helix inversion steps. The rate of rotation of **1b** was found to be consistent with previously reported motors with related structures, indicating that introduction of a PBI moiety does not exert significant influence on the light-driven rotary motion of motor **1b**. Besides, the tetra-acid functionalized motor **1b** was assembled onto an amine-coated quartz surface. UV−vis studies on surfaces revealed the successful attachment and the preserved light-driven rotation of **1b**. The optimized motor **1b** has been subjected to defocused wide-field imaging, and the dynamics of individual light-driven molecular motor molecules on surfaces were studied in detail the result of which have been presented in a separated report.[66] Our recent studies demonstrate that, by a careful design, a molecular motor with multiple components is able to be assembled on surfaces and its rotary function can be preserved. The studies of the architecture and functioning of multicomponent motors in particular interactions between the chromophore and motor core provide important guidelines for further design of more advanced molecular motors and machines.

EXPERIMENTAL SECTION

General Remarks. All reagents were obtained from commercial sources and used as received without further purification. Solvents for extraction and chromatography were technical grade. All solvents used in reactions were freshly distilled from appropriate drying agents before use. All reactions were performed under an inert atmosphere (Ar). Analytical TLC was performed with Merck silica gel 60 F254 plates, and visualization was accomplished by UV light. Flash chromatography was carried out using Merck silica gel 60 (230−400 mesh ASTM). Solvents for spectroscopic studies were of spectrophotometric grade. ^{1}H NMR spectra were recorded on 400 and 500 MHz NMR spectrometers. ^{13}C NMR spectra were recorded on 100 and 125 MHz NMR spectrometers. The deuterated solvents (CD_2Cl_2 and $CDCl_3$) were treated with Na_2CO_3 and molecular sieves (4 Å) and degassed by argon prior to use. Chemical shifts are denoted in parts per million (ppm) relative to the residual solvent peak (CD_2Cl_2: ^{1}H δ = 5.32 ppm, ^{13}C δ = 53.84 ppm; $CDCl_3$: ^{1}H δ = 7.26 ppm, ^{13}C δ = 77.0 ppm). The splitting parameters are designated as follows: s = singlet, d = doublet, t = triplet, q = quartet, m = multiplet, dd = doublet of doublets. High-resolution mass spectrometry (ESIMS) was performed on an LTQ Orbitrap XL mass spectrometer with ESI ionization. MALDI-TOF spectra were obtained with a Voyager DE-Pro instrument. UV/vis measurements were performed using a 1 cm quartz cuvette. UV irradiation experiments were carried out using an ENB-280C/FE lamp.

Syntheses. *6-Iodo-2-methyl-2,3-dihydro-1H-cyclopenta[a]-naphthalen-1-one (**6**).* In a sealed tube containing **5**[20] (640 mg, 2.3 mmol), CuI (219 mg, 1.1 mmol), and NaI (3.44 g, 23 mmol) were added dry 1,4-dioxane (50 mL) and *N*,*N*′-dimethyl ethylenediamine (202 mg, 2.3 mmol). The mixture was stirred at 140 °C for 24 h. The solvent was removed *in vacuo*, and the material was purified by flash chromatography (SiO_2, pentane/EtOAc = 10:1) to give the product as a yellow sticky oil (642 mg, 91%). ^{1}H NMR (400 MHz, $CDCl_3$) δ 9.23 (d, J = 8.3 Hz, 1H), 8.35 (d, J = 8.7 Hz, 1H), 8.14 (d, J = 7.4 Hz, 1H), 7.57 (d, J = 8.7 Hz, 1H), 7.42−7.31 (m, 1H), 3.50 (dd, J = 18.3, 8.1 Hz, 1H), 2.97−2.73 (m, 2H), 1.38 (d, J = 7.3 Hz, 3H). ^{13}C NMR (101 MHz, $CDCl_3$) δ 153.0, 148.0, 140.0, 135.9, 132.7, 131.5, 128.5, 127.1, 126.9, 122.3, 121.0, 45.4, 29.7, 19.3. HRMS (ESI-TOF) m/z: [M + H]$^+$ calcd for $C_{14}H_{11}IO$ 322.9933; found 322.9951.

*Motor **3**.* To a solution of ketone **6** (219 mg, 0.68 mmol) in toluene (10 mL), Lawesson's reagent (415 mg, 1.1 mmol) was added. The mixture was stirred at reflux for 2 h, and the solvent was subsequently evaporated. The residue was purified by flash column (SiO_2, pentane/ethyl acetate = 30:1) to obtain a blue solution of the corresponding thioketone. A THF solution (20 mL) of diazo compound **7**[56](476 mg, 1.37 mmol) was added, and the diazo-thioketone mixture was heated at reflux overnight. The solvent was then evaporated, and the residue was purified by chromatography (SiO_2, pentane/CH_2Cl_2 = 10:1) to yield motor **3** (250 mg, 50%) as a red solid. Mp: 79−81 °C; ^{1}H NMR (400 MHz, $CDCl_3$) δ 8.57 (d, J = 8.4 Hz, 1H), 7.92 (d, J = 1.8 Hz, 1H), 7.81 (d, J = 9.1 Hz, 3H), 7.78−7.60 (m, 3H), 7.52 (dd, J = 8.4, 1.8 Hz, 1H), 7.37−7.21 (m, 1H), 6.93 (dd, J = 8.5, 1.9 Hz, 1H), 6.53 (d, J = 8.5 Hz, 1H), 4.36−4.18 (m, 1H), 3.69−3.55 (m, 1H), 2.78 (d, J = 15.3 Hz, 1H), 1.36 (d, J = 6.7 Hz, 3H). ^{13}C NMR (101 MHz, $CDCl_3$) δ 151.8, 148.6, 140.2, 138.4, 137.4, 136.4, 135.7, 135.6, 133.3, 130.3, 130.3, 130.2, 129.3, 129.2, 127.9, 127.8, 126.8, 125.6, 125.3, 123.1, 122.4, 121.2, 100.3, 45.7, 41.6, 29.7, 19.1. HRMS (ESI-TOF) m/z: [M + H]$^+$ calcd for $C_{27}H_{18}Br_2I$ 626.8742; found 626.8710.

*Motor **8**.* To a mixture of **3** (165 mg, 0.26 mmol), $Pd(PPh_3)_2Cl_2$ (2.5 mol %), and CuI (5 mol %) were added dry and degassed THF (10 mL) and $(i\text{-Pr})_2NH$ (2 mL). After the mixture was stirred at rt for 10 min, triisopropylsilyl acetylene (42 mg, 0.27 mmol) was added. The mixture was stirred for 15 h and then poured into aqueous NH_4Cl solution. After extraction with CH_2Cl_2 (3 × 20 mL), the combined organic layers were washed with brine and dried (Na_2SO_4). The solvent was removed, and the residue was purified by flash chromatography (SiO_2, pentane/CH_2Cl_2 = 10:1) to yield **8** as a brown oil (171 mg, 99%). ^{1}H NMR (400 MHz, $CDCl_3$) δ 8.57 (d, J = 8.4 Hz, 1H), 7.92 (d, J = 1.9 Hz, 1H), 7.87−7.76 (m, 3H), 7.70 (ddd, J = 14.1, 7.8, 3.4 Hz, 4H), 7.52 (m, 2H), 7.35−7.17 (m, 2H), 6.93 (dd, J = 8.4, 2.0 Hz, 1H), 6.53 (d, J = 8.5 Hz, 1H), 4.35−4.16 (m, 1H), 3.58 (dd, J = 15.3, 5.6 Hz, 1H), 2.78 (d, J = 15.3 Hz, 1H), 1.36 (d, J = 6.7 Hz, 3H), 1.23 (d, J = 2.7 Hz, 18H). ^{13}C NMR (126 MHz, $CDCl_3$) δ 156.8, 156.6, 155.9, 152.1, 144.5, 144.0, 141.2, 140.2, 138.6, 138.5, 138.4, 137.4, 137.4, 137.3, 136.4, 135.7, 135.6, 131.1, 130.4, 129.4, 129.3, 127.9, 127.8, 127.7, 127.3, 126.8, 125.6, 125.3, 126.7, 125.6, 125.3, 123.1, 122.4, 121.2, 100.3, 93.5, 93.1, 45.8, 43.9, 31.8, 31.8, 16.7, 2.6. HRMS (ESI-TOF) m/z: [M + H]$^+$ calcd for $C_{38}H_{39}Br_2Si$ 681.1188; found 681.1203.

*Motor **9**.* A mixture of **8** (161 mg, 0.24 mmol), pinacol ester **4** (240 mg, 0.71 mmol), K_3PO_4 (300 mg, 1.44 mmol), and $Pd(PPh_3)_4$ (98 mg, 0.096 mmol) in 1,4-dioxane (20 mL) was stirred at 90 °C for 16 h. After the mixture was cooled to rt, it was diluted with ethyl acetate (30 mL) and filtered. Following removal of the solvent, the residue was purified by flash column chromatography (SiO_2, pentane/CH_2Cl_2 = 1:6) to yield ester **9** as a brown oil (156 mg, 56%). ^{1}H NMR (400 MHz, $CDCl_3$) δ 8.64 (d, J = 1.4 Hz, 3H), 8.51 (dd, J = 3.5, 1.6 Hz, 2H), 8.22 (t, J = 2.2 Hz, 1H), 8.15−8.04 (m, 3H), 7.85−7.67 (m, 6H), 7.35−7.28 (m, 2H), 7.20−7.12 (m, 2H), 6.81 (d, J = 8.3 Hz, 1H), 4.39 (s, 1H), 4.03−3.94 (m, 12H), 3.68−3.59 (m, 1H), 2.83 (d, J = 15.2 Hz, 1H), 1.44 (d, J = 6.6 Hz, 3H), 1.24 (d, J = 2.7 Hz, 18H). ^{13}C NMR (100 MHz, $CDCl_3$) δ 167.2, 167.1, 156.8, 156.8, 156.6, 155.9, 152.1, 144.5, 144.0, 141.2, 140.2, 138.6, 138.5, 138.4, 137.4, 137.4, 137.3, 136.4, 135.7, 135.6, 131.1, 130.4, 130.3, 130.3, 130.2, 130.2, 129.4, 129.3, 127.9, 127.8, 127.7, 127.3, 126.8, 125.6, 125.3, 126.7, 125.6, 125.3, 123.1, 122.4, 121.2, 100.3, 93.5, 93.1, 53.4, 45.8, 43.9, 31.8, 31.8, 16.7, 2.6. HRMS (ESI-TOF) m/z: [M + H]$^+$ calcd for $C_{58}H_{57}O_8Si$ 909.3823; found 909.3847.

*Motor **10**.* To a solution of **9** (120 mg, 0.13 mmol) in THF (10 mL) at 0 °C TBAF (0.1 mL) was added. The mixture was stirred at 0

DOI: 10.1021/acs.joc.8b00654
J. Org. Chem. 2018, 83, 6025−6034

°C for 1 h and then poured into aqueous NH_4Cl solution. After extraction with $CHCl_3$ (3 × 10 mL), the combined organic layers were washed with brine and dried (Na_2SO_4). The solvent was removed, and the residue was purified by flash chromatography (SiO_2, pentane/ethyl acetate = 1:3) to yield **10** as a dark red oil (116 mg, 95%). ^{1}H NMR (400 MHz, $CDCl_3$) δ 9.05 (d, J = 1.8 Hz, 1H), 8.63 (d, J = 1.7 Hz, 2H), 8.36 (d, J = 8.6 Hz, 1H), 7.97 (d, J = 5.0 Hz, 1H), 7.89−7.81 (m, 1H), 7.80−7.71 (m, 1H), 7.65 (d, J = 7.6 Hz, 2H), 7.57 (s, 1H), 7.47−7.38 (m, 1H), 7.22 (t, J = 7.4 Hz, 1H), 7.09 (t, J = 7.5 Hz, 2H), 6.96 (s, 2H), 6.80 (d, J = 7.7 Hz, 1H), 6.65 (d, J = 7.9 Hz, 1H), 4.39−4.25 (m, 1H), 4.00 (m, 12H), 3.57 (dd, J = 15.0, 6.0 Hz, 1H), 2.74 (d, J = 15.2 Hz, 1H), 2.18 (s, 1H), 1.39 (d, J = 6.8 Hz, 3H). ^{13}C NMR (126 MHz, $CDCl_3$) δ 167.2, 167.1, 156.8, 156.6, 155.9, 152.1, 144.5, 144.0, 141.2, 140.2, 138.6, 138.5, 138.4, 137.4, 137.3, 136.4, 135.7, 135.6, 131.1, 130.4, 130.3, 130.2, 130.2, 129.4, 129.3, 127.9, 127.8, 127.7, 127.3, 126.8, 126.7, 125.6, 125.3, 125.6, 125.3, 123.1, 122.4, 121.2, 100.3, 93.5, 93.1, 53.4, 45.8, 43.9, 31.8, 31.8, 16.7. HRMS (ESI-TOF) m/z: $[M + H]^+$ calcd for $C_{49}H_{37}O_8$ 753.2410; found 753.2438.

Motor ***11***. To a mixture of motor **10** (75 mg, 0.10 mmol), PBI **2**[59] (68 mg, 0.10 mmol), $Pd(PPh_3)_2Cl_2$ (2.5 mol %), and CuI (5 mol %) were added dry and degassed THF (10 mL) and $(i\text{-Pr})_2NH$ (2 mL). The mixture was stirred overnight and then poured into aqueous NH_4Cl solution. After extraction with $CHCl_3$ (3 × 20 mL), the combined organic layers were washed with brine and dried (Na_2SO_4). The solvent was removed, and the residue was purified by flash chromatography (SiO_2, $CHCl_3$) to yield motor **11** as a dark red solid (66 mg, 57%). Mp > 200 °C; ^{1}H NMR (400 MHz, $CDCl_3$) δ 8.77−8.61 (m, 10H), 8.36 (d, J = 8.5 Hz, 1H), 7.96 (dd, J = 6.5, 2.4 Hz, 1H), 7.92−7.89 (m, 2H), 7.85−7.82 (m, 1H), 7.77−7.73 (m, 1H), 7.63 (t, J = 0.9 Hz, 2H), 7.56 (d, J = 1.6 Hz, 1H), 7.39 (ddd, J = 7.4, 2.9, 1.7 Hz, 2H), 7.23−7.18 (m, 1H), 7.11−7.06 (m, 4H), 6.95 (d, J = 7.5 Hz, 2H), 6.78 (dd, J = 8.1, 7.1 Hz, 1H), 6.65 (d, J = 7.9 Hz, 1H), 5.18 (d, J = 5.5 Hz, 1H), 4.37−4.32 (m, 1H), 3.96 (s, 12H), 3.61−3.55 (m, 1H), 2.74 (d, J = 15.2 Hz, 1H), 1.93−1.82 (m, 3H), 1.39 (d, J = 6.6 Hz, 3H), 1.36−1.14 (m, 18H), 0.86−0.77 (m, 6H).^{13}C NMR (126 MHz, $CDCl_3$) δ 167.2, 167.1, 156.8, 156.6, 155.9, 152.1, 144.5, 144.0, 141.2, 137.4, 137.4, 137.3, 136.4, 135.7, 135.6, 135.6, 132.9, 131.1, 130.4, 129.4, 127.7, 127.3, 126.7, 120.8, 120.4, 120.0, 119.6, 117.1, 116.3, 115.9, 115.5, 103.8, 102.7, 93.5, 93.1, 72.7, 72.6, 72.3, 72.1, 53.4, 52.3, 52.2, 45.2, 43.9, 34.3, 34.2, 34.2, 34.2, 32.0, 31.9, 31.8, 31.8, 28.4, 28.3, 28.3, 28.3, 25.3, 25.3, 25.3, 25.2, 21.9, 16.7, 16.7. HRMS (ESI-TOF) m/z: calcd for $C_{92}H_{75}N_2O_{12}$ $[M + H]^+$ 1399.5242; found 1399.5287.

Motor ***1a***. Ester **11** (90 mg, 0.067 mmol) was dissolved in THF (5 mL), MeOH (5 mL), and $NaOH_{(aq.)}$ (1 M, 5 mL), and the mixture was heated at 75 °C for 6 h. Subsequently the mixture was cooled to rt, and water (5 mL) was added. THF and MeOH were removed by rotary evaporation. A brown precipitate was formed upon titration of the mixture with $HCl_{(aq.)}$ (1 M) until pH = 2. After filtration, the brown solid was washed with cold water (10 mL) and dried *in vacuo*, affording motor **1a** as a brown solid (65 mg, 75%). Mp > 200 °C; ^{1}H NMR (500 MHz, CD_2Cl_2) δ 8.77−8.61 (m, 10H), 8.36 (d, J = 8.5 Hz, 1H), 7.96 (dd, J = 6.5, 2.4 Hz, 1H), 7.92−7.89 (m, 2H), 7.85−7.82 (m, 1H), 7.77−7.73 (m, 1H), 7.63 (t, J = 0.9 Hz, 2H), 7.56 (d, J = 1.6 Hz, 1H), 7.39 (ddd, J = 7.4, 2.9, 1.7 Hz, 2H), 7.23−7.18 (m, 1H), 7.11−7.06 (m, 4H), 6.95 (d, J = 7.5 Hz, 2H), 6.78 (dd, J = 8.1, 7.1 Hz, 1H), 6.65 (d, J = 7.9 Hz, 1H), 5.18 (d, J = 5.5 Hz, 1H), 4.37−4.32 (m, 1H), 3.61−3.55 (m, 1H), 2.74 (d, J = 15.2 Hz, 1H), 1.93−1.82 (m, 3H), 1.39 (d, J = 6.6 Hz, 3H), 1.36−1.14 (m, 18H), 0.86−0.77 (m, 6H). ^{13}C NMR (101 MHz, $CDCl_3$) δ 167.2, 167.1, 156.8, 156.6, 155.9, 152.1, 144.5, 144.0, 141.2, 137.4, 137.4, 137.3, 136.4, 135.7, 135.6, 135.6, 132.9, 131.1, 130.4, 129.4, 127.7, 127.3, 126.7, 120.8, 120.4, 120.0, 119.6, 117.1, 116.3, 115.9, 115.5, 103.8, 102.7, 93.5, 93.1, 72.7, 72.6, 72.3, 72.1, 45.2, 43.9, 34.3, 34.2, 34.2, 34.2, 32.0, 31.9, 31.8, 31.8, 28.4, 28.3, 28.3, 28.3, 25.3, 25.3, 25.3, 25.2, 21.9, 16.7, 16.7. HRMS (ESI-TOF) m/z: calcd for $C_{88}H_{67}N_2O_{12}$ $[M + H]^+$ 1344.4616; found 1344.4602.

Rigid Linker ***13***. To a mixture of **12** (452 mg, 0.40 mmol), PBI **2** (272 mg, 0.40 mmol), $Pd(PPh_3)_2Cl_2$ (2.5 mol %), and CuI (5 mol %) were added dry and degassed THF (25 mL) and $(i\text{-Pr})_2NH$ (5 mL). The mixture was stirred for 15 h and then poured into aqueous NH_4Cl solution. After extraction with $CHCl_3$ (3 × 20 mL), the combined organic layer was washed with brine and dried (Na_2SO_4). The solvent was removed, and the residue was purified by flash chromatography (SiO_2, $CHCl_3$) to yield PBI **13** as a dark red solid (431 mg, 65%). Mp > 200 °C; ^{1}H NMR (400 MHz, $CDCl_3$) δ 8.63 (dd, J = 45.0, 7.9 Hz, 8H), 7.73 (d, J = 8.4 Hz, 2H), 7.38 (d, J = 8.4 Hz, 2H), 7.14−6.88 (m, 10H), 5.19 (d, J = 5.7 Hz, 1H), 3.99 (m, 16H), 2.34−2.18 (m, 3H), 1.85 (m, 16H), 1.41−1.16 (m, 18H), 1.10 (m, 22H), 0.83 (t, J = 6.9 Hz, 6H). ^{13}C NMR (101 MHz, $CDCl_3$) δ 163.4, 154.1, 153.7, 153.4, 153.3, 135.1, 134.8, 134.2, 132.5, 131.8, 129.7, 129.5, 128.8, 126.6, 126.3, 124.3, 123.3, 123.1, 123.1, 117.4, 117.3, 117.2, 114.6, 114.4, 113.7, 100.1, 94.2, 91.6, 71.2, 71.1, 71.0, 54.8, 32.4, 31.8, 29.7, 29.2, 27.0, 22.8, 22.7, 22.7, 22.6, 14.1, 10.6, 10.6, 10.6, 10.5. MALDI-TOF m/z: calcd for $C_{105}H_{104}N_2O_{12}$ M^+ 1584.7589; found 1584.7578.

Motor ***14***. To a mixture of motor **10** (76 mg, 0.10 mmol), $Pd(PPh_3)_2Cl_2$ (2.5 mol %), CuI (5 mol %), and PDI **13** (165 mg, 0.10 mmol) were added dry and degassed THF (10 mL) and $(i\text{-Pr})_2NH$ (2 mL). The mixture was stirred overnight and then poured into aqueous NH_4Cl solution. After extraction with $CHCl_3$ (3 × 20 mL), the combined organic layers were washed with brine and dried (Na_2SO_4). The solvent was removed, and the residue was purified by flash chromatography (SiO_2, $CHCl_3$) to yield motor **14** as a dark red solid (118 mg, 58%). Mp > 200 °C; ^{1}H NMR (400 MHz, $CDCl_3$) δ 8.74 (d, J = 8.5 Hz, 1H), 8.72−8.49 (m, 8H), 8.08 (d, J = 1.8 Hz, 1H), 8.03−7.94 (m, 1H), 7.89−7.81 (m, 3H), 7.73 (d, J = 7.9 Hz, 3H), 7.54 (d, J = 8.1 Hz, 2H), 7.38 (dt, J = 9.4, 3.6 Hz, 4H), 7.21 (d, J = 7.4 Hz, 1H), 7.09−6.96 (m, 10H), 6.79 (s, 1H), 6.79−6.63 (m, 3H), 5.23−5.16 (m, 1H), 4.40−4.32 (m, 1H), 4.03 (m, 20H), 3.57 (d, J = 5.6 Hz, 1H), 2.78 (d, J = 15.0 Hz, 1H), 2.29−2.20 (m, 2H), 2.11−2.00 (m, 2H), 1.88 (td, J = 7.1, 3.2 Hz, 20H), 1.49−0.93 (m, 50H), 0.87−0.78 (m, 6H). ^{13}C NMR (100 MHz, $CDCl_3$) δ 174.2, 155.7, 154.8, 152.9, 138.7, 136.3, 135.7, 132.2, 131.8, 131.7, 127.8, 126.4, 126.3, 126.0, 125.4, 125.2, 124.6, 124.2, 123.6, 122.8, 121.6, 120.8, 120.4, 120.0, 119.5, 109.4, 109.2, 105.0, 69.0, 68.9, 68.7, 60.3, 51.4, 36.6, 34.1, 31.9, 30.5, 29.7, 29.7, 29.6, 29.6, 29.6, 29.6, 29.5, 29.5, 29.5, 29.4, 29.4, 29.3, 29.2, 29.1, 26.1, 26.1, 26.0, 25.0, 22.7, 21.0, 18.3, 14.3, 14.2. MALDI-TOF: calcd for $C_{156}H_{142}N_2O_{20}$ M^+ 2363.0156; found 2363.0179.

Motor ***1b***. Ester **14** (90 mg, 0.038 mmol) was dissolved in THF (5 mL), MeOH (5 mL) and $NaOH_{(aq.)}$ (1 M, 5 mL), and the mixture was heated at 75 °C for 16 h. The mixture was cooled to rt, and water (5 mL) was added. THF and MeOH were removed by rotary evaporation. A brown precipitate was formed upon titration of the mixture with $HCl_{(aq.)}$ (1 M) until pH = 1. After filtration, the brown solid was washed with cold water (10 mL) and dried *in vacuo*, affording motor **1b** as a brown solid (55 mg, 85%). Mp > 200 °C; ^{1}H NMR (400 MHz, $CDCl_3$) δ 8.74−8.60 (m, 11H), 7.98 (dd, J = 6.0, 3.1 Hz, 1H), 7.94−7.87 (m, 3H), 7.86−7.80 (m, 2H), 7.74 (d, J = 7.5 Hz, 1H), 7.55 (ddd, J = 8.3, 6.8, 1.3 Hz, 1H), 7.43−7.33 (m, 2H), 7.21 (td, J = 7.4, 1.1 Hz, 3H), 7.15−7.07 (m, 4H), 7.06−6.98 (m, 3H), 6.79 (td, J = 7.6, 1.2 Hz, 1H), 6.70 (d, J = 7.9 Hz, 1H), 5.19 (m, 3H), 4.33 (q, J = 6.5 Hz, 1H), 4.12−3.93 (m, 8H), 3.58 (dd, J = 15.0, 5.7 Hz, 1H), 2.77 (d, J = 15.0 Hz, 1H), 2.24 (dd, J = 9.6, 4.1 Hz, 4H), 2.02 (m, 2H), 1.96−1.74 (m, 20H), 1.66−0.98 (m, 50H), 0.86−0.79 (m, 7H). ^{13}C NMR (126 MHz, CD_2Cl_2) δ 182.0, 157.5, 156.6, 154.8, 141.0, 138.3, 137.7, 133.9, 133.6, 133.6, 130.0, 128.3, 128.0, 127.9, 127.3, 126.8, 126.3, 126.3, 125.8, 124.7, 123.3, 121.4, 120.8, 120.4, 120.0, 111.4, 111.3, 111.0, 109.4, 109.2, 106.9, 106.8, 71.0, 71.0, 70.6, 38.5, 38.4, 35.9, 33.9, 32.4, 31.6, 31.6, 31.6, 31.5, 31.5, 31.4, 31.3, 31.3, 31.27, 31.2, 31.1, 31.1, 31.0, 28.1, 28.0, 27.9, 26.6, 24.6, 19.9, 19.8, 15.8. MALDI-TOF m/z: calcd for $C_{152}H_{134}N_2O_{20}$ 2306.9530; found 2306.9588.

Preparation of Motor Functionalized Monolayer MS-1b. Quartz slides (Ted Pella, Inc.) were cleaned by immersing in a piranha solution (3/7 ratio of 30% H_2O_2 in H_2SO_4) at 90 °C for 1 h and rinsed copiously first with doubly distilled water (3 times) and then with MeOH and dried under a stream of N_2 before surface modification. The piranha-cleaned quartz slides were silanized[56] by immersing in a 1 mm solution of 3-aminopropyl(diethoxy)methylsilane in freshly distilled toluene at rt for 12 h, then rinsed copiously with toluene and MeOH, sonicated first in toluene and then in MeOH,

DOI: 10.1021/acs.joc.8b00654
J. Org. Chem. 2018, 83, 6025−6034

and dried under a stream of argon. The amine-coated slides were immersed in a DMF solution of **1b** (10^{-4} M) at rt for 12 h, and then the slides were washed with DMF, water, and MeOH and then dried under a stream of argon.

■ ASSOCIATED CONTENT

Supporting Information

The Supporting Information is available free of charge on the ACS Publications website at DOI: 10.1021/acs.joc.8b00654.

Kinetic studies of **1b** in solution by UV−vis absorption spectroscopy, NMR spectra of new compounds (PDF)

■ AUTHOR INFORMATION

Corresponding Authors

*E-mail: j.chen@rug.nl.
*E-mail: b.l.feringa@rug.nl.

ORCID

Jiawen Chen: 0000-0002-0251-8976
Ben L. Feringa: 0000-0003-0588-8435

Notes

The authors declare no competing financial interest.

■ ACKNOWLEDGMENTS

This work was supported financially by The Netherlands Organization for Scientific Research (NWO-CW), the European Research Council (ERC; Advanced Grant No. 694345 to B.L.F.), and the Ministry of Education, Culture and Science (Gravitation Program No. 024.001.035). Dr. Sander J. Wezenberg is acknowledged for helpful discussions and manuscript correction.

■ REFERENCES

(1) Berg, J. M.; Tynoczko, J. L.; Styer, L. *Biochemistry*, 5th ed.; W. H. Freeman: New York, 2006.
(2) Schliwa, M. *Molecular Motors*; Wiley-VCH: Weinheim, Germany, 2003.
(3) Boyer, P. D. Molecular Motors: What Makes ATP Synthase Spin? *Nature* **1999**, *402*, 247−249.
(4) Bray, D. *Cell Movements: From Molecules to Motility*; Garland, New York, 1992.
(5) Hess, H.; Vogel, V. Molecular Shuttles Based on Motor Proteins: Active Transport in Synthetic Environments. *Rev. Mol. Biotechnol.* **2001**, *82*, 67−85.
(6) Stoddart, J. F. Molecular Machines. *Acc. Chem. Res.* **2001**, *34*, 410−411.
(7) Sauvage, J.-P., Ed. *Molecular Machines and Motors*; Springer: Berlin, 2001.
(8) Kinbara, K.; Aida, T. Toward Intelligent Molecular Machines: Directed Motions of Biological and Artificial Molecules and Assemblies. *Chem. Rev.* **2005**, *105*, 1377−1400.
(9) Kottas, G. S.; Clarke, I. L.; Horinek, D.; Michl, J. Artificial Molecular Rotors. *Chem. Rev.* **2005**, *105*, 1281−1376.
(10) Wang, Y.; Li, Q. Light-Driven Chiral Molecular Switches or Motors in Liquid Crystals. *Adv. Mater.* **2012**, *24*, 1926−1945.
(11) Li, Q., Ed. *Intelligent Stimuli Responsive Materials: From Well-defined Nanostructures to Applications*; John Wiley & Sons: Hoboken, NJ, 2013.
(12) Kay, E. R.; Leigh, D. A.; Zerbetto, F. Synthetic Molecular Motors and Mechanical Machines. *Angew. Chem., Int. Ed.* **2007**, *46*, 72−191.
(13) Erbas-Cakmak, S.; Leigh, D. A.; McTernan, C. T.; Nussbaumer, A. L. Artificial Molecular Machines. *Chem. Rev.* **2015**, *115*, 10081−10206.
(14) Balzani, V.; Venturi, M.; Credi, A. *Molecular Devices and Machines - A Journey into the Nanoworld*; Wiley-VCH: Weinheim, 2003.
(15) Watson, M. A.; Cockroft, S. L. Man-made Molecular Machines: Membrane Bound. *Chem. Soc. Rev.* **2016**, *45*, 6118−6129.
(16) Kassem, S.; van Leeuwen, T.; Lubbe, A. S.; Wilson, M. R.; Feringa, B. L.; Leigh, D. A. Artificial Molecular Motors. *Chem. Soc. Rev.* **2017**, *46*, 2592−2621.
(17) Bisoyi, H. K.; Li, Q. Light-Driven Liquid Crystalline Materials: From Photo-Induced Phase Transitions and Property Modulations to Applications. *Chem. Rev.* **2016**, *116*, 15089−15166.
(18) Zheng, Z. G.; Li, Y.; Bisoyi, H. K.; Wang, L.; Bunning, T. J.; Li, Q. Three-dimensional Control of the Helical Axis of A Chiral Nematic Liquid Crystal by Light. *Nature* **2016**, *531*, 352−356.
(19) Koumura, N.; Geertsema, E. M.; van Gelder, M. B.; Meetsma, A.; Feringa, B. L. Second Generation Light-Driven Molecular Motors. Unidirectional Rotation Controlled by a Single Stereogenic Center with Near-Perfect Photoequilibria and Acceleration of the Speed of Rotation by Structural Modification. *J. Am. Chem. Soc.* **2002**, *124*, 5037−5051.
(20) Feringa, B. L. The Art of Building Small: From Molecular Switches to Motors (Nobel Lecture). *Angew. Chem., Int. Ed.* **2017**, *56*, 11060−11078.
(21) Wang, J.; Feringa, B. L. Dynamic Control of Chiral Space in A Catalytic Asymmetric Aeaction Using A Molecular Motor. *Science* **2011**, *331*, 1429−1432.
(22) Kudernac, T.; Ruangsupapichat, N.; Parschau, M.; Macia, B.; Katsonis, N.; Harutyunyan, S. R.; Ernst, K. H.; Feringa, B. L. Electrically Driven Directional Motion of A Four-wheeled Molecule on A Metal Surface. *Nature* **2011**, *479*, 208−211.
(23) García-López, V.; Chen, F.; Nilewski, L. G.; Duret, G.; Aliyan, A.; Kolomeisky, A. B.; Robinson, J. T.; Wang, G.; Pal, R.; Tour, J. M. Molecular Machines Open Cell Membranes. *Nature* **2017**, *548*, 567−572.
(24) Li, Q.; Fuks, G.; Moulin, E.; Maaloum, M.; Rawiso, M.; Kulic, I.; Foy, J. T.; Giuseppone, N. Macroscopic Contraction of A Gel Induced By the Integrated Motion of Light-driven Molecular Motors. *Nat. Nanotechnol.* **2015**, *10*, 161−165.
(25) Eelkema, R.; Pollard, M. M.; Vicario, J.; Katsonis, N.; Ramon, B. S.; Bastiaansen, C. W. M.; Broer, D. J.; Feringa, B. L. Nanomotor Rotates Microscale Objects. *Nature* **2006**, *440*, 163.
(26) Asshoff, S. J.; Iamsaard, S.; Bosco, A.; Cornelissen, J. J. L. M.; Feringa, B. L.; Katsonis, N. Time-programmed Helix Inversion in Phototunable Liquid Crystals. *Chem. Commun.* **2013**, *49*, 4256−4258.
(27) Zhao, D. P.; van Leeuwen, T.; Cheng, J. L.; Feringa, B. L. Dynamic Control of Chirality and Self-assembly of Double-stranded Helicates With Light. *Nat. Chem.* **2017**, *9*, 250−256.
(28) Chen, J.; Leung, F. K.-C.; Stuart, M. C. A.; Kajitani, T.; Fukushima, T.; van der Giessen, E.; Feringa, B. L. Artificial Muscle-like Function From Hierarchical Supramolecular Assembly of Photo-responsive Molecular Motors. *Nat. Chem.* **2017**, *10*, 132−138.
(29) Astumian, R. D. Thermodynamics and Kinetics of a Brownian Motor. *Science* **1997**, *276*, 917−922.
(30) Coskun, A.; Banaszak, M.; Astumian, R. D.; Stoddart, J. F.; Grzybowski, B. A. Great Expectations: Can Artificial Molecular Machines Deliver On Their Promise? *Chem. Soc. Rev.* **2012**, *41*, 19−30.
(31) Ulman, A. Formation and Structure of Self-Assembled Monolayers. *Chem. Rev.* **1996**, *96*, 1533−1554.
(32) Ciampi, S.; Harper, J. B.; Gooding, J. J. Wet Chemical Routes to the Assembly of Organic Monolayers on Silicon Surfaces via the Formation of Si-C Bonds: Surface Preparation, Passivation and Functionalization. *Chem. Soc. Rev.* **2010**, *39*, 2158−2183.
(33) Haensch, C.; Hoeppener, S.; Schubert, U. S. Chemical Modification of Self-assembled Silane Based Monolayers by Surface Reactions. *Chem. Soc. Rev.* **2010**, *39*, 2323−2334.
(34) Balzani, V.; Credi, A.; Venturi, M. Molecular Machines Working on Surfaces and at Interfaces. *ChemPhysChem* **2008**, *9*, 202−220.

DOI: 10.1021/acs.joc.8b00654
J. Org. Chem. 2018, 83, 6025−6034

(35) van Delden, R. A.; ter Wiel, M. K. J.; Pollard, M. M.; Vicario, J.; Koumura, N.; Feringa, B. L. Unidirectional Molecular Motor on a Gold Surface. *Nature* **2005**, *437*, 1337−1340.
(36) Pollard, M. M.; Lubomska, M.; Rudolf, P.; Feringa, B. L. Controlled Rotary Motion in a Monolayer of Molecular Motors. *Angew. Chem., Int. Ed.* **2007**, *46*, 1278−1280.
(37) Noji, H.; Yasuda, R.; Yoshida, M.; Kinosita, K., Jr Direct Observation of the Rotation of F1-ATPase. *Nature* **1997**, *386*, 299−302.
(38) Hutchison, J. A.; Uji-i, H.; Deres, A.; Vosch, T.; Rocha, S.; Müller, S.; Bastian, A. A.; Enderlein, J.; Nourouzi, H.; Li, C.; Herrmann, A.; Müllen, K.; De Schryver, F.; Hofkens, J. A surface-bound molecule that undergoes optically biased Brownian rotation. *Nat. Nanotechnol.* **2014**, *9*, 131−136.
(39) Haugland, R. P. *Handbook of Fluorescent Probes and Research Chemicals*; Molecular Probes, Inc.: Eugene, OR, 1989.
(40) Jancy, B.; Asha, S. K. Control of Molecular Structure in the Generation of Highly Luminescent Liquid Crystalline Perylenebisimide Derivatives: Synthesis, Liquid Crystalline and Photophysical Properties. *J. Phys. Chem. B* **2006**, *110*, 20937−20947.
(41) Würthner, F.; Saha-Möller, C. R.; Fimmel, B.; Ogi, S.; Leowanawat, P.; Schmidt, D. Perylene Bisimide Dye Assemblies as Archetype Functional Supramolecular Materials. *Chem. Rev.* **2016**, *116*, 962−1052.
(42) Zollinger, H. *Color Chemistry*; VCH Verlagsgesellschaft: Weinheim, 1987.
(43) Herrmann, A.; Müllen, K. From Industrial Colorants to Single Photon Sources and Biolabels: The Fascination and Function of Rylene Dyes. *Chem. Lett.* **2006**, *35*, 978−985.
(44) Petritsch, K.; Dittmer, J. J.; Marseglia, E. A.; Friend, R. H.; Lux, A.; Rozenberg, G. G.; Moratti, S. C.; Holmes, A. B. Dye-based Donor/Acceptor Solar Cells. *Sol. Energy Mater. Sol. Cells* **2000**, *61*, 63−72.
(45) Schmidt-Mende, L.; Fechtenkotter, A.; Mullen, K.; Moons, E.; Friend, R. H.; MacKenzie, J. D. Self-organized Discotic Liquid Crystals for High-efficiency Organic Photovoltaics. *Science* **2001**, *293*, 1119−1122.
(46) Angadi, M. A.; Gosztola, D.; Wasielewski, M. R. Organic Light Emitting Diodes Using Poly (phenylenevinylene) Doped With Perylenediimide Electron Acceptors. *Mater. Sci. Eng., B* **1999**, *63*, 191−194.
(47) Kraft, A.; Grimsdale, A. C.; Holmes, A. B. Electroluminescent Conjugated Polymers-Seeing Polymers in a New Light. *Angew. Chem., Int. Ed.* **1998**, *37*, 402−428.
(48) Ranke, P.; Bleyl, I.; Simmerer, J.; Haarer, D.; Bacher, A.; Schmidt, H. W. Electroluminescence and Electron Transport in a Perylene Dye. *Appl. Phys. Lett.* **1997**, *71*, 1332−1334.
(49) Kalinowski, J.; Di Marco, P. D.; Fattori, L.; Cocchi, M. Voltage-induced Evolution of Emission Spectra in Organic Light-emitting Diodes. *J. Appl. Phys.* **1998**, *83*, 4242−4248.
(50) Katz, H. E.; Bao, Z.; Gilat, S. L. Synthetic Chemistry for Ultrapure, Processable, and High-mobility Organic Transistor Semiconductors. *Acc. Chem. Res.* **2001**, *34*, 359−369.
(51) Würthner, F. Plastic Transistors Reach Maturity for Mass Applications in Microelectronics. *Angew. Chem., Int. Ed.* **2001**, *40*, 1037−1039.
(52) Chen, Z. J.; Debije, M. G.; Debaerdemaeker, T.; Osswald, P.; Würthner, F. Tetrachloro-substituted Perylene Bisimide Dyes As Promising n-type Organic Semiconductors: Studies on Structural, Electrochemical and Charge Transport Properties. *ChemPhysChem* **2004**, *5*, 137−140.
(53) Vosch, T.; Hofkens, J.; Cotlet, M.; Kohn, F.; Fujiwara, H.; Gronheid, R.; Van Der Biest, K; Weil, T.; Herrmann, A.; Mullen, K.; Mukamel, S.; Van der Auweraer, M.; De Schryver, F. C. Influence of Structural and Rotational Isomerism on the Triplet Blinking of Individual Dendrimer Molecules. *Angew. Chem., Int. Ed.* **2001**, *40*, 4643−4648.
(54) Gronheid, R.; Hofkens, J.; Kohn, F.; Weil, T.; Reuther, E.; Müllen, K.; De Schryver, F. C. Intramolecular Förster Energy Transfer in a Dendritic System at the Single Molecule Level. *J. Am. Chem. Soc.* **2002**, *124*, 2418−2419.
(55) Wang, J.; Kulago, A.; Browne, W. R.; Feringa, B. L. Photoswitchable Intramolecular H-stacking of Perylenebisimide. *J. Am. Chem. Soc.* **2010**, *132*, 4191−4196.
(56) Chen, J.; Chen, K. Y.; Carroll, G. T.; Feringa, B. L. Facile Assembly of Light-driven Molecular Motors Onto a Solid Surface. Chem. *Chem. Commun.* **2014**, *50*, 12641−12644.
(57) Klapars, A.; Buchwald, S. L. Copper-catalyzed Halogen Exchange in Aryl halides: an Aromatic Finkelstein Reaction. *J. Am. Chem. Soc.* **2002**, *124*, 14844−14845.
(58) Xue, M.; Zhu, G.; Li, Y.; Zhao, X.; Jin, Z.; Kang, E.; Qiu, S. Structure, Hydrogen Storage, and Luminescence Properties of Three 3D Metal− Organic Frameworks with NbO and PtS Topologies. *Cryst. Growth Des.* **2008**, *8*, 2478−2483.
(59) Robb, M. J.; Newton, B.; Fors, B. P.; Hawker, C. J. One-Step Synthesis of Unsymmetrical N-Alkyl-N-aryl Perylene Diimides. *J. Org. Chem.* **2014**, *79*, 6360−6365.
(60) Vicario, J.; Walko, M.; Meetsma, A.; Feringa, B. L. Fine Tuning of the Rotary Motion by Structural Modification in Light-driven Unidirectional Molecular Motors. *J. Am. Chem. Soc.* **2006**, *128*, 5127−5135.
(61) Lor, M.; Thielemans, J.; Viaene, L.; Cotlet, M.; Hofkens, J.; Weil, T.; Hampel, C.; Müllen, K.; Van der Auweraer, M.; De Schryver, F. C. Photoinduced Electron Transfer in a Rigid First Generation Triphenylamine Core Dendrimer Substituted with a Peryleneimide Acceptor. *J. Am. Chem. Soc.* **2002**, *124*, 9918−9925.
(62) Liu, R.; Holman, M. W.; Zang, L.; Adams, D. M. Single-molecule Spectroscopy of Intramolecular Electron Transfer in Donor-bridge-acceptor Systems. *J. Phys. Chem. A* **2003**, *107*, 6522−6526.
(63) Berberich, M.; Krause, A. M.; Orlandi, M.; Scandola, F.; Wurthner, F. *Angew. Chem., Int. Ed.* **2008**, *47*, 6616−6619.
(64) Ziener, U.; Godt, A. Synthesis and Characterization of Monodisperse Oligo(phenyleneethynylene)s. *J. Org. Chem.* **1997**, *62*, 6137−6143.
(65) Chen, J.; Kistemaker, J. C. M.; Robertus, J.; Feringa, B. L. Molecular Stirrers in Action. *J. Am. Chem. Soc.* **2014**, *136*, 14924−14932.
(66) Krajnik, B.; Chen, J.; Watson, M. A.; Cockroft, S. L.; Feringa, B. L.; Hofkens, J. Defocused Imaging of UV-Driven Surface-Bound Molecular Motors. *J. Am. Chem. Soc.* **2017**, *139*, 7156−7159.

DOI: 10.1021/acs.joc.8b00654
J. Org. Chem. 2018, 83, 6025−6034